Acta Biomaterialia (2012)

Contents lists available at SciVerse ScienceDirect

Acta Biomaterialia

journal homepage: www.elsevier.com/locate/actabiomat

# Anti-infective and osteointegration properties of silicon nitride, poly(ether ether ketone), and titanium implants

T.J. Webster [a], A.A. Patel [b], M.N. Rahaman [c], B. Sonny Bal [d,*]

[a] School of Engineering and Department of Orthopaedics, Brown University, Providence, RI 02917, USA
[b] Department of Orthopaedic Surgery and Rehabilitation, Loyola University Medical Center, Maywood, IL 60153, USA
[c] Department of Materials Science and Engineering, Missouri University of Science and Technology, Rolla, MO 65409, USA
[d] Department of Orthopaedic Surgery, School of Medicine, University of Missouri, Columbia, MO 65211, USA



ARTICLE INFO

*Article history:*
Received 24 May 2012
Received in revised form 19 July 2012
Accepted 25 July 2012
Available online xxxx

*Keywords:*
Silicon nitride
Poly(ether ether ketone)
Titanium
Orthopedic implants

ABSTRACT

Silicon nitride ($Si_3N_4$) is an industrial ceramic used in spinal fusion and maxillofacial reconstruction. Maximizing bone formation and minimizing bacterial infection are desirable attributes in orthopedic implants designed to adhere to living bone. This study has compared these attributes of $Si_3N_4$ implants with implants made from two other orthopedic biomaterials, i.e. poly(ether ether ketone) (PEEK) and titanium (Ti). Dense implants made of $Si_3N_4$, PEEK, or Ti were surgically implanted into matching rat calvarial defects. Bacterial infection was induced with an injection of $1 \times 10^4$ *Staphylococcus epidermidis*. Control animals received saline only. On 3, 7, and 14 days, and 3 months post-surgery four rats per time period and material were killed, and calvariae were examined to quantify new bone formation and the presence or absence of bacteria. Quantitative evaluation of osteointegration to adjacent bone was done by measuring the resistance to implant push-out (n = 8 rats each for Ti and PEEK, and n = 16 rats for $Si_3N_4$). Three months after surgery in the absence of bacterial injection new bone formation around $Si_3N_4$ was ~69%, compared with 24% and 36% for PEEK and Ti, respectively. In the presence of bacteria new bone formation for $Si_3N_4$, Ti, and PEEK was 41%, 26%, and 21%, respectively. Live bacteria were identified around PEEK (88%) and Ti (21%) implants, whereas none were present adjacent to $Si_3N_4$. Push-out strength testing demonstrated statistically superior bone growth onto $Si_3N_4$ compared with Ti and PEEK. $Si_3N_4$ bioceramic implants demonstrated superior new bone formation and resistance to bacterial infection compared with Ti and PEEK.



## 1. Introduction

Silicon nitride ($Si_3N_4$) is a synthetic non-oxide ceramic that is used in many industrial applications, and has been investigated or adapted as a biomedical material since 1989 [1–14]. The rationale for using $Si_3N_4$-based implants in skeletal reconstruction is based on its favorable combination of mechanical strength, microstructure, and cytotoxicity [11,12,15]. Polished and porous implants made of $Si_3N_4$ have shown encouraging outcomes in spine and maxillofacial surgery [11,13]. In contrast to the limited clinical experience with $Si_3N_4$, implants made of titanium (Ti) and its alloys have been used in skeletal reconstruction for many decades [16,17]. More recently, poly(ether ether ketone) (PEEK), a polymer with modest strength and a low modulus of elasticity compared with metal, has been investigated as an orthopedic biomaterial [18,19] and is commonly used in spine surgery [20].

Long-term, stable fixation of orthopedic implants to skeletal bone relies on direct in-growth of host bone into the textured implant surface. Implant failure and clinical symptoms of pain can follow if such bone in-growth does not occur. A serious problem that can complicate an otherwise well-fixed and properly functioning implant is bacterial infection, which can manifest itself immediately after surgery or even years later. Implant-related infections usually require extensive surgical debridement, implant extraction, and prolonged antibiotic treatment [21,22]. Implant surfaces can accumulate serum proteins that can promote bacterial adhesion and colonization [23]. Adherent bacteria such as *Staphylococcus epidermidis* are known to synthesize a complex surrounding biofilm layer that is impervious to host immune surveillance and systemic antibiotic therapy [23–25]. Therefore, resistance to bacterial infection would be a very desirable material property in orthopedic implants. To date, however, all implant materials are susceptible to bacterial seeding in vivo.

The purpose of this investigation was to test the potential antimicrobial properties and osteointegration capability of dense $Si_3N_4$ implants in an animal model. For comparison we used two common

* Corresponding author. Tel.: +1 573 882 6762; fax: +1 573 882 8200.
*E-mail address:* balb@health.missouri.edu (B. Sonny Bal).

1742-7061/$ - see front matter © 2012 Acta Materialia Inc. Published by Elsevier Ltd. All rights reserved.
http://dx.doi.org/10.1016/j.actbio.2012.07.038

**Table 1**
Comparative properties of medical grades of $Si_3N_4$, ASTM grade 4 titanium and Invibio PEEK Optima®.

| Property | Units | $Si_3N_4$ | Ti – ASTM Grade 4 | PEEK Optima® |
|---|---|---|---|---|
| Composition | NA | $Si_3N_4$, $Y_2O_3$, $Al_2O_3$ | Chemically Pure | Chemically Pure |
| Surface Composition | NA | $SiNH_2$ and SiOH | $TiO_2$ Layer | –OH Groups |
| Surface Roughness (AFM) | nm | 25.3 | 3.06 | 1 |
| Isoelectric Point | NA | 9 | ~4.5 | ~4.5 |
| Surface Charge at pH = 7 | NA | Positive | Negative | Negative |
| Sessile Water Drop Wetting Angle | Degrees | 39 | 76 | 95 |



orthopedic biomaterials, Ti and PEEK. The null hypothesis was that $Si_3N_4$, Ti, and PEEK would demonstrate identical properties in terms of bacterial infection and bone growth onto implant surfaces.

## 2. Materials and methods

### 2.1. Biomaterials

The materials used in this study included medical grades of $Si_3N_4$ (Amedica Corp., Salt Lake City, UT), ASTM grade 4 titanium (Fisher Scientific, Continental Steel & Tube Co., Fort Lauderdale, FL) and PEEK Optima® (Invibio, Thornton Cleveleys, UK). The $Si_3N_4$ provided by Amedica was produced using sintering with hot isostatic pressing with $Al_2O_3$ and $Y_2O_3$ as densification additives, similar to methods previously reported by Iturriza et al. [26]. All samples were sterilized using ultraviolet light exposure for 24 h on all sides. The relevant properties of these three materials are given in Table 1.

The surfaces of the three materials were characterized for morphology and roughness by scanning electron microscopy (SEM) using a LEO 1530 VP FE-4800 field emission gun scanning electron microscope (Zeiss, Peabody, MA). The results are shown in Fig. 1. All three materials were used in the as-received condition. The PEEK and medical grade Ti samples had machined surfaces, whereas the $Si_3N_4$ ceramic was as-fired. SEM images of PEEK and Ti reveal a macro-rough surface typical of machined components. However, the as-fired $Si_3N_4$ implant material possessed nanostructured surface features with a larger total surface area compared with Ti and PEEK. Sessile water drop tests using a Krüss Easy Drop Contact Angle instrument (Germany) with analysis by the Drop Shape Analysis program (v.1.8) were performed on each material to assess their wetting characteristics (Table 1) [27].

### 2.2. Calvarial defect model

Ninety six skeletally mature Wistar rats (350–450 g) underwent treatment using an experimental protocol that was approved by the Institutional Animal Care and Use Committee. Animals were housed and cared for in accordance with standard guidelines in a facility accredited by the Association for the Assessment and Accreditation of Laboratory Animal Care, according to the policies and principles established by the Animal Welfare Act and the NIH Guide for Care and Use of Laboratory Animals. Prior to surgery the animals were administered atropine sulfate (0.05 mg $kg^{-1}$ subcutaneously) 15–30 min before induction of anesthesia using ketamine (40–80 mg $kg^{-1}$ intraperitoneally). All surgery was performed under aseptic conditions, with a sterile surgical field, surgical gown, cap, mask, sterile gloves, and sterile instruments. Immediately prior to surgery the surgical site was shaved and disinfected topically with Betadine scrubs. Using magnification and high intensity illumination a full thickness incision was made from the nasofrontal area to the external occipital protuberance along the mid-sagittal plane, permitting reflection and exposure of the calvarium. Under constant copious irrigation with saline a trephine bur was used to create critical sized elliptical through-and-through defects in the parietal bones, measuring larger than the $10 \times 10 \times 1.75$ mm implants [28]. Trephined bone was carefully removed to avoid injury to the underlying dura.

Defects were randomly reconstituted with test coupons of either Ti (n = 24), or PEEK (n = 24), or $Si_3N_4$ (n = 48). Prior to closure the surgical site in half of the animals receiving each biomaterial was randomly inoculated with a standard aliquot of $1 \times 10^4$ *S. epidermidis* (ATCC, Manassas, VA, strain no. 35984). The other half received a matching aliquot of saline as a control. After surgical repair of the wound the animals were individually caged under a warming lamp and intermittently turned from side to side. The animals were administered buprenorphine (0.02 mg $kg^{-1}$ intramuscularly) as an analgesic for 3–5 days post-operatively. The surgical sites were monitored daily for untoward swelling or signs of infection. At least three animals (for each biomaterial and bacteria/saline group) were killed at 3, 7, and 14 days, and 3 months post-surgery via $CO_2$ administration and cervical dislocation.

### 2.3. Specimen preparation

Block sections of the calvarium were harvested from the surgical sites and fixed in 10% neutral buffered formalin. After exposing the area the calvarium was resected with a high-speed handpiece. A thin layer of cerebral tissue was excised with a scalpel. The remaining tissue was left attached to the inner face of the cranium in order to prevent damage to the implantation area. Upon receipt

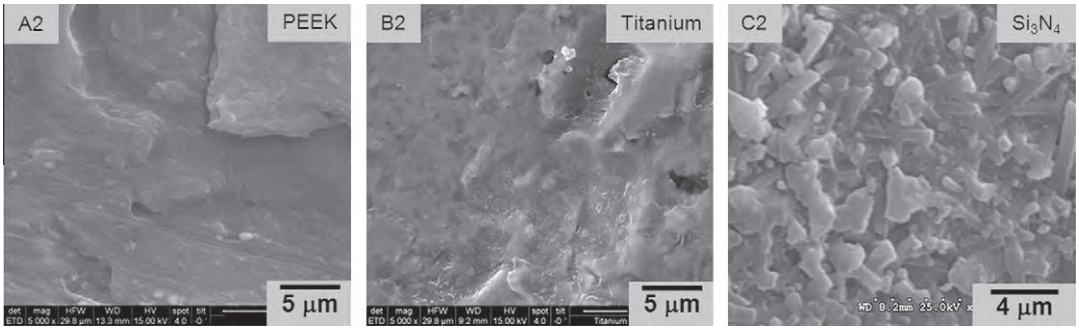


**Fig. 1.** SEM surface microstructures of PEEK Optima®, titanium and silicon nitride.

in the laboratory the specimens were immediately dehydrated with a graded series of alcohol for 9 days. Following dehydration the specimens were infiltrated with a light curing embedding resin (Technovit 7200 VLC, Kulzer, Wehrheim, Germany). After 20 days infiltration with constant shaking at normal atmospheric pressure the specimens were embedded and polymerized by 450 nm light, with the temperature of the specimens never exceeding 40 °C. The specimens were then prepared by the cutting/grinding method of Donath to expose the implant surface and juxtaposed tissue for subsequent staining as described below [29,30].

### 2.4. Histomorphometry

The top section from each surgical defect was evaluated morphometrically. Specimens were fixed in 10% neutral buffered formalin and demineralized in 10% ethylene diamine tetraacetic acid. Skull samples were excised so that every experimental and control area was separated and embedded in paraffin. Sections were cut, stained with Masson–Goldner trichrome stain (for new bone growth) and a modified gram stain (for bacteria) and examined with a light microscope. The exact boundaries of the original defects were determined using light microscopy. Digital photomicrographs of the defects permitted a precise calculation of the proportion of the original defect filled with new bone and/or biofilm formation. All measurements were made by an examiner who was blind with respect to treatment.

### 2.5. Mechanical testing

Upon sample thawing push-out tests were conducted to evaluate the functional mechanical integration of the constructs into the host calvaria, performed in a Micro Tester 5848 (Instron) with a 1 kN load cell. A 1 mm diameter indenter probe was fabricated for the test. Thus the push-out test measured the strength required to push the sample out along the direction of potential new bone growth on the sample side containing the features. A schematic diagram of the push-out test is shown in Fig. 2.

### 2.6. Bacterial infection and bone growth

At the time of death samples with adjacent tissue were removed and stained for *S. epidermidis* biofilm formation using a modified gram stain (yellow in the histology images). Histology was quantified for the number of bacteria in the implant area and juxtaposed to the implant. Sections were measured semi-quantitatively using Bioquant image analysis software (Nashville, TN). Images of the sections were taken with an Olympus BX5I microscope connected to a CCD camera using the same light intensity and exposure. Similarly, new bone was quantified from sectioned planes by selecting a fixed threshold for positive Masson–Goldner trichrome stain (purple in the histology images) and calculating the positive pixel area per stain divided by the total area available for bone in-growth. These values are reported as a percentage of bone area per defect area (outlined by a pink circle in the histology images).

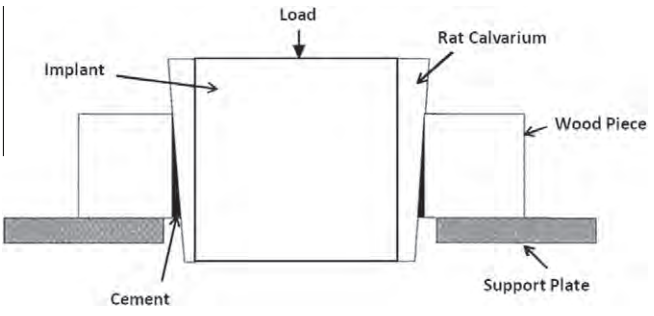


**Fig. 2.** Schematic of the method used to determine push-out strengths.

### 2.7. Justification for species and sample size

Wistar rats were chosen for this study because the calvarial defect model has been extensively studied in this species for bone healing and remodeling [28–31]. The minimum number of animals per study group was chosen based on pre-study statistical power analysis derived from a previous study on the same species in our laboratory that indicated a minimum sample size of four rats per group (unpublished data). No animals were lost in this experimental protocol, resulting in the minimum sample size per group available for data analysis.

Histology was performed on one rat at each time point for Ti and PEEK (with and without inoculation) and two rats at each time point for $Si_3N_4$ (with and without inoculation). This totaled 32 animals. Push-out tests were also performed on two rats at each time point for Ti and PEEK (with and without inoculation) and four rats at each time point for $Si_3N_4$ (with and without inoculation). This totaled 64 animals. The total number of animals was 96.

### 2.8. Statistical analysis

Quantitative statistical analysis and hypothesis testing was conducted by fitting the mechanical push-out strength data to a simplified Poisson–Boltzman equation [32] of the form:

$$S = S_0 \left\{1 - \exp\left[-\left(\frac{t}{\tau_0}\right)\right]\right\}$$

where S is the push-out strength at a given time, t is time, $S_0$ is the maximum push-out strength, and $\tau_0$ is the characteristic time at which a significant portion (>60%) of the maximum strength is achieved.

Hypothesis testing was completed using nonlinear regression analysis and confidence intervals in accordance with the techniques described by Brown [33]. A $P$ value of <0.05 was deemed statistically significant.

## 3. Results

The histomorphological and mechanical test results of the study are presented in Tables 2 and 3 and Figs. 3–6. Table 2 provides data for observations without bacterial inoculation at the site of implantation. Table 3 shows comparative results when each implant was inoculated with $10^4$ *S. epidermidis*. Figs. 3 and 5 provide quantitative analyses and statistical inference testing for the push-out tests. Comparative histological sections are shown in Figs. 4 and 6 for implants with and without bacterial inoculation, respectively, 90 days after surgery.

Under the no bacteria condition the PEEK and Ti implants were structurally unstable and were unable to provide adequate histological sections at the 3 and 7 days time periods (Table 2). This is because insufficient tissue formed around the implants, and they could not be sectioned. Conversely, $Si_3N_4$ implants were stable due to sufficient juxtaposed tissue growth and showed reasonable osteointegration even at these short time points. The percentage regenerated bone at the implant interface and within the surgical defect for $Si_3N_4$ implants were 4% and 20% and 18% and 30% for 3 and 7 days after surgery, respectively.

14 days post-operative the observed bone growth at all implant interfaces was amenable to measurement. The results were 2%, 7% and 31% for PEEK, Ti and $Si_3N_4$, respectively. This subsequently increased, such that at the 90 days time point osteointegration of

**Table 2**
Wistar rat calvaria histology and push-out strengths without bacterial inoculation.

| Observation | Time Interval (Days) | | | |
|---|---|---|---|---|
| | 3 | 7 | 14 | 90 |
| *% of Bone at Implant Interface* | | | | |
| PEEK | Unstable | Unstable | 2 | 8 |
| Titanium | Unstable | Unstable | 7 | 19 |
| Silicon Nitride | 4 ± 1 | 20 ± 1 | 31 ± 8 | 59 ± 7 |
| *% of Bone Within Surgical Area* | | | | |
| PEEK | Unstable | Unstable | 14 | 24 |
| Titanium | Unstable | Unstable | 11 | 36 |
| Silicon Nitride | 18 ± 2 | 30 ± 2 | 50 ± 1 | 69 ± 4 |
| *Implant Push Out Strength (MPa)* | | | | |
| PEEK | .11 ± .01 | .14 ± .03 | .16 ± .01 | .26 ± .01 |
| Titanium | .25 ± .00 | .30 ± .00 | .30 ± .00 | .36 ± .01 |
| Silicon Nitride | .29 ± .02 | .36 ± .01 | .63 ± .07 | .71 ± .02 |

For histological observations of PEEK and Ti $n = 1$, for $Si_3N_4$ $n = 2$. For push-out strengths of PEEK and Ti $n = 2$, for $Si_3N_4$ $n = 4$. Error values are standard errors of the mean (SEM).

**Table 3**
Wistar rat calvaria histology and push-out strengths with bacterial inoculation.

| Observation | Time Interval (Days) | | | |
|---|---|---|---|---|
| | 3 | 7 | 14 | 90 |
| *% of Bone at Implant Interface* | | | | |
| PEEK | Unstable | Unstable | 0 | 5 |
| Titanium | Unstable | Unstable | 1 | 9 |
| Silicon Nitride | Unstable | Unstable | 8 ± 5 | 23 ± 2 |
| *% of Bacteria at Implant Interface* | | | | |
| PEEK | Unstable | Unstable | NM | 95 |
| Titanium | Unstable | Unstable | 75 | 67 |
| Silicon Nitride | Unstable | Unstable | 25 ± 3 | 0 ± 0 |
| *% of Bone Within Surgical Area* | | | | |
| PEEK | Unstable | Unstable | 2 | 21 |
| Titanium | Unstable | Unstable | 9 | 26 |
| Silicon Nitride | Unstable | Unstable | 27 ± 2 | 41 ± 2 |
| *% of Bacteria Within Surgical Area* | | | | |
| PEEK | Unstable | Unstable | 25 | 88 |
| Titanium | Unstable | Unstable | 45 | 21 |
| Silicon Nitride | Unstable | Unstable | 13 ± 2 | 0 ± 0 |
| *Implant Push Out Strength (MPa)* | | | | |
| PEEK | 0 ± 0 | 0 ± 0 | 0 ± 0 | 0 ± 0 |
| Titanium | 0 ± 0 | 0 ± 0 | .03 ± .03 | .04 ± .01 |
| Silicon Nitride | .10 ± .01 | .14 ± .03 | .25 ± .02 | .26 ± .00 |

For histological observations of PEEK and Ti $n = 1$, for $Si_3N_4$ $n = 2$. For push-out strengths of PEEK and Ti $n = 2$, for $Si_3N_4$ $n = 4$. Error values are standard errors of the mean (SEM).

PEEK, Ti and $Si_3N_4$ was 8%, 19% and 59%, respectively. Similar trends were observed for the percentage of new bone formation within the calvarial defect. The amount of regenerated bone associated with $Si_3N_4$ implants was essentially two- to three-times that of the other two implant materials at 3 months after operation (Table 2).

Despite the lack of histological results for PEEK and Ti at the short time intervals, push-out strength testing was possible for all implants under the no bacterial inoculation condition. The results are presented in Table 2 and Fig. 3. $Si_3N_4$ had the highest push-out strength of all implant materials at each time point, and the increase in strength was more than double the other two implant materials at the 90 days observation point. Strength differences between $Si_3N_4$ and the other two implant materials were statistically significant ($P < 0.01$) at the 14 and 90 days time periods. Although the push-out strength of Ti 90 days after surgery was lower than that of $Si_3N_4$, it was still better than that of PEEK (Fig. 4).

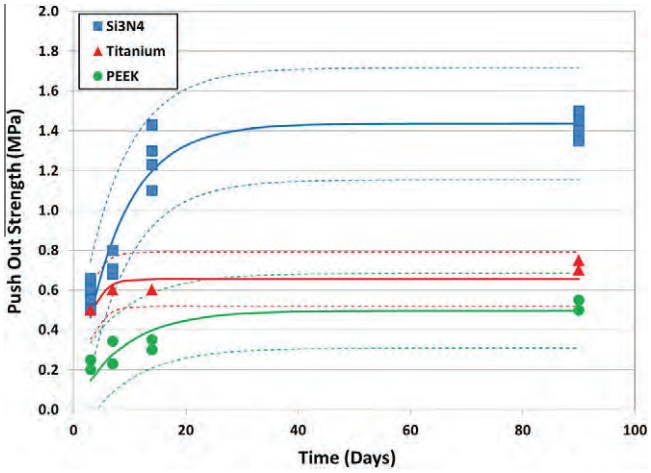


**Fig. 3.** Implant push-out strengths without bacterial inoculation: Nonlinear regression analysis using the simplified Boltzmann equation. Dashed lines represent 95% confidence interval.

The histological sections of these implants without bacterial inoculation 90 days post-operative indicated that all three materials exhibited reasonable in vivo behavior and were well tolerated by the animals (Fig. 4). There was minimal indication of inflammation and no infection. Bone growth into the calvarial defect occurred with all three materials, but was more pronounced for $Si_3N_4$, as shown in the histological sections.

Histological observations of the inoculated implants were attempted at the 3 and 7 days time points, but all three biomaterials were unstable. Histological studies could only be performed on post-operative days 14 and 90 (Table 3). PEEK and Ti implants inoculated with bacteria showed no or minimal osteointegration, regardless of the implantation time. For $Si_3N_4$ significantly greater new bone formation occurred in the calvarial defects, including material in-growth, compared with Ti and PEEK at all implantation times. Specifically, 3 months after surgery the amounts of new bone at the implant interface and within the surgical defect were 5%, 9% and 23%, and 21%, 26% and 41%, for PEEK, Ti and $Si_3N_4$, respectively.

The $Si_3N_4$ implants also exhibited considerably decreased bacterial biofilm formation compared with that of PEEK and Ti. 90 days post-implantation live bacteria were present in the calvariae with PEEK (88%) and Ti implants (21%), while no bacteria could be identified in defects containing $Si_3N_4$ implants (Table 3 and Fig. 5). The histological results were consistent with the bacteriostatic characteristics of $Si_3N_4$, along with its ability to promote new bone formation.

Even in specimens inoculated with bacteria mechanical testing showed significantly greater push-out strengths for $Si_3N_4$ implants compared with PEEK and Ti implants. 90 days post-implantation push-out strengths for $Si_3N_4$ were over fivefold greater than the values observed for Ti and PEEK ($P < 0.01$). Push-out strengths for Ti implants were statistically greater than PEEK 90 days post-operative, but this difference was not statistically significant ($P = 0.10$). All of these results were consistent with the histological findings shown in Fig. 6.

## 4. Discussion

Relatively low rates of $Si_3N_4$ spinal implant infections (0.01%) have been observed in clinical surveillance by a manufacturer of such implants (personal communication, R. Wolfarth, Director of Regulatory Affairs, Amedica Corp.). This rate is less than the

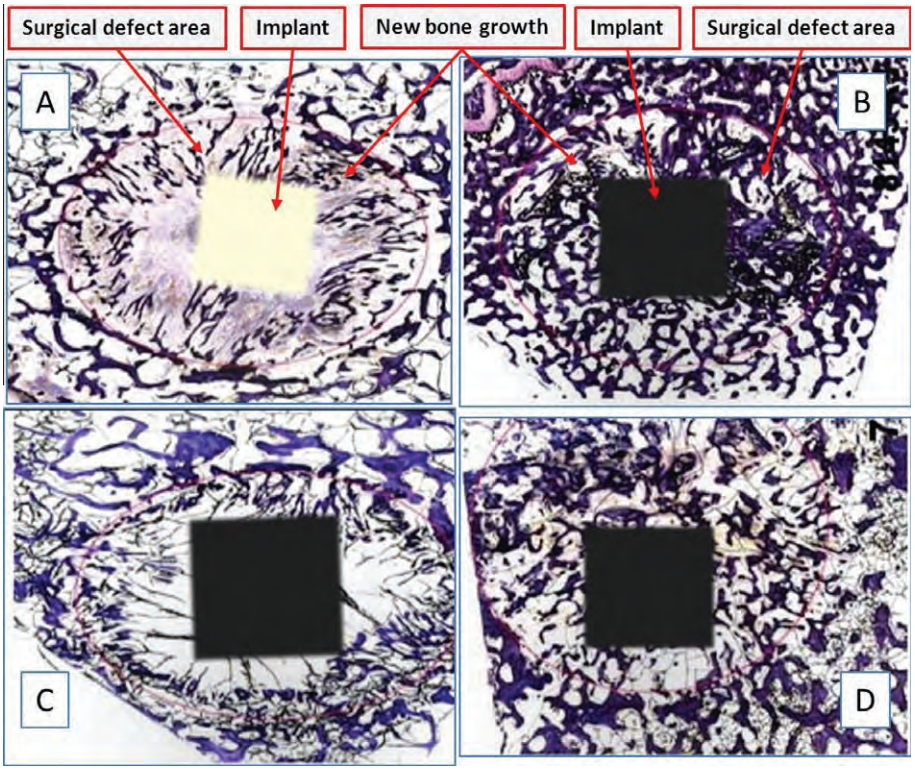


**Fig. 4.** Wistar rat calvaria histology 3 months after implantation without bacterial inoculation: (A) PEEK, 8% new bone at implant interface, 24% new bone in surgical area; (B) $Si_3N_4$, 65% new bone at implant interface, 71% new bone in surgical area; (C) Ti, 19% new bone at implant interface, 36% new bone in surgical area; (D) $Si_3N_4$, 52% new bone at implant interface, 66% new bone in surgical area.

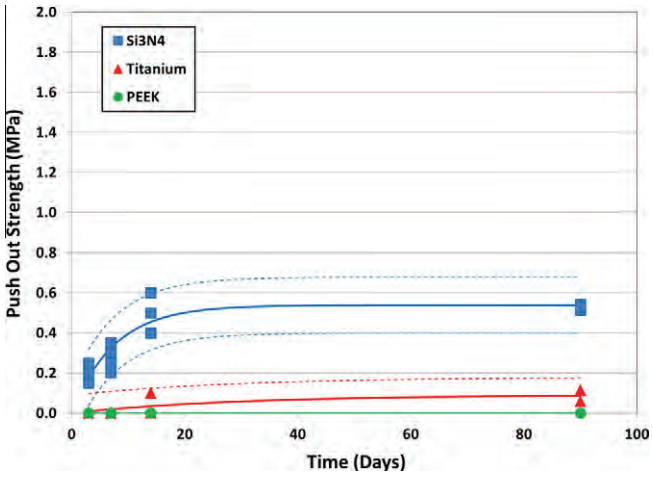


**Fig. 5.** Implant push-out strengths with bacterial inoculation: Nonlinear regression analysis using the simplified Boltzmann equation. Dashed lines represent 95% confidence interval.

expected frequency of infection for prosthetic total hip implants (2.6–4.0%) and prosthetic total knee implants (3.5–4.0%) cited in the literature [21–23]. Ti-based alloys are commonly used in the manufacture of both total hip and total knee implants. In spinal surgery implants made of metal as well as PEEK are used extensively [17,19,34], and clinical reports have shown surgical site infection rates of between 0.9% and 5.4% following spine surgery. [35–37] Given these data, we sought to test the null hypothesis that resistance to *S. epidermidis*-induced bacterial infection would not differ between $Si_3N_4$, Ti, and PEEK. We found instead that $Si_3N_4$ demonstrated anti-infective properties, as well as superior attachment to host bone in vivo, compared with Ti and PEEK.

Bacterial adhesion to biomaterials is a complex multifactorial process that depends on variables such as surface roughness, chemical composition, wettability, and the bacterial species [23,38]. Surface adhesion of bacteria is necessary for sustained periprosthetic infection to be manifest. Serum proteins such as albumin, fibronectin, fibrinogen, laminin, denatured collagen, and others can promote or inhibit bacterial adhesion to a substratum surface [25,39]. One reason why *S. epidermidis*-induced sepsis did not occur around $Si_3N_4$ in the present study may be the greater surface wettability or hydrophilicity of $Si_3N_4$ compared with PEEK and Ti (Table 1). Changes in surface wettability can influence the initial protein adsorption and conformation, which in turn can also influence subsequent bacterial and bone cell responses [40,41].

Surface adsorbed serum proteins can suppress the initial adhesion of *S. epidermidis*, and the formation of mature bacterial biofilm is also impeded on hydrophilic surfaces [42]. Surface modification of polymers has, for example, been shown to alter the adherence of *S. epidermidis* such that hydrophilic surfaces show less non-specific adhesion of bacteria compared with control surfaces. [43]. As a non-oxide ceramic material $Si_3N_4$ has a very hydrophilic surface, and selective protein adsorption may have rendered its surface relatively resistant to bacterial adhesion, thereby leading to the observations in the present study.

Other factors that may explain the observed behavior of $Si_3N_4$ probably relate to its net positive surface charge and the presence of amine groups at the implant surface. These properties may have led to an effect that is comparable to chitosan, a known bactericidal polymer coating for orthopedic implants [44]. It has been suggested that the interaction of negatively charged bacteria with positively charged amine groups leads to bacterial membrane disruption and lysis [45]. The same material and surface characteristics contribute to pronounced attachment and proliferation of osteoblasts, presumably due to differences in cell membrane composition, size and

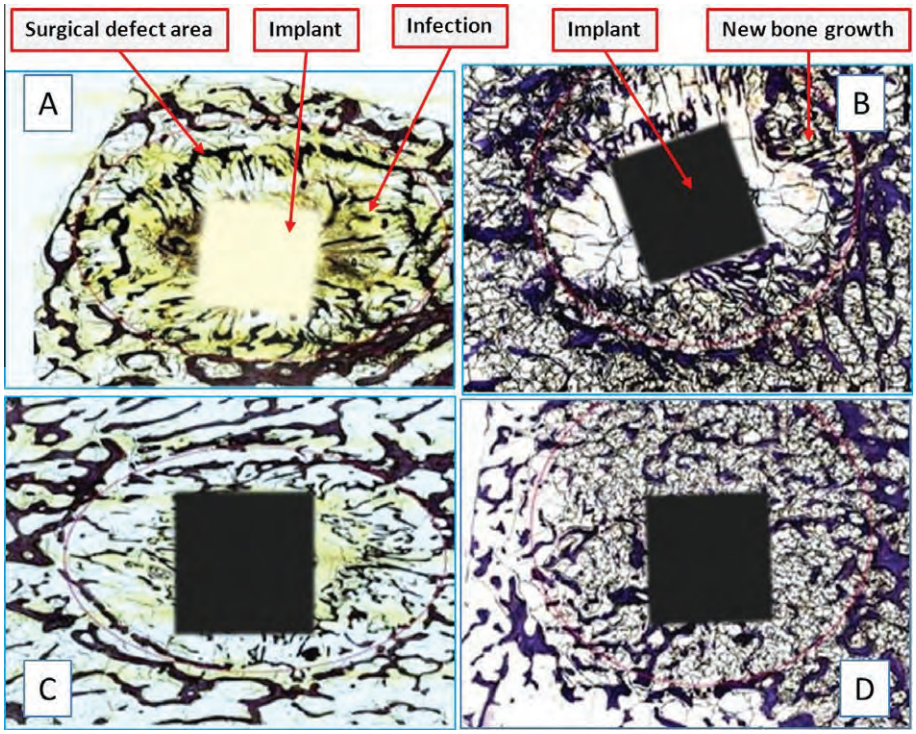


**Fig. 6.** Wistar rat calvaria histology 3 months after implantation with bacterial inoculation: (A) PEEK, 5% new bone at implant interface, 95% bacteria at implant interface, 21% new bone growth in surgical area, 88% bacterial growth in surgical area; (B) $Si_3N_4$, 25% new bone at implant interface, 0% bacteria at implant interface, 39% new bone growth in surgical area, 0% bacteria in surgical area; (C) Ti, 9% bone at implant interface, 67% bacteria at implant interface, 26% new bone growth in surgical area, 21% bacteria in surgical area; (D) $Si_3N_4$, 21% new bone at implant interface, 0% bacteria at implant interface, 42% new bone growth in surgical area, 0% bacteria in surgical area.

morphological differences between bacteria and osteoblasts [46,47]. Further research is needed to confirm whether $Si_3N_4$ surface properties are operative mechanisms for the observed in vivo antibacterial and osteoinductive characteristics.

The bone formation results around $Si_3N_4$, Ti, and PEEK may reflect different rates of cell attachment and growth between these biomaterials. Fibroblasts and osteoblasts adhere differently to PEEK, Ti, cobalt–chrome alloys, and ultra-high molecular weight polyethylene [48]. These differences reflect variations in the surface topography and micro/nanotexture of the respective biomaterials. For example, during bone healing osteoblasts mature in areas where osteoclast activity creates a micron/nanoscale roughness and the appropriate surface texture for bone formation [49]. In commercially pure titanium substrates micron- and submicron- and nanoscale features promote greater osteoblast differentiation, matrix deposition, and production of osteogenic growth factors [50,51] compared with smooth surfaces [52]. Other studies have shown that cells on titanium and titanium alloys are more differentiated than cells on traditional cell culture plastic [53,54]. Therefore, differences in surface chemistry and surface micro/nanotexture could explain the different rates of bone formation around Ti, PEEK, and $Si_3N_4$ implants in the present experiments.

The PEEK implants used in this study did not have any surface treatments. Untreated PEEK promotes osteoblast and fibroblast attachment and cell proliferation without adversely influencing cell growth [55]. To enhance osteoblastic differentiation PEEK coatings such as hydroxyapatite, tricalcium phosphate, diamond-like carbon, and Ti may be necessary [19,56]. In vivo studies showing osseous fusion and restoration of biomechanical properties in the spine have relied on PEEK implants augmented with bone autograft or rhBMP-2 on a collagen sponge, rather than PEEK alone [20]. Despite comparable contact angles and material wettability between PEEK and rough Ti alloy substrates, osteoblasts cultured on Ti present a more mature phenotype than cells cultured on PEEK [57]. These observations may explain the relatively low push-out strength observed in the present study with PEEK, and suggest that PEEK implants with bioactive coatings may have fared better. However, bioactive coatings may also render PEEK more susceptible to infection. For instance, hydroxyapatite-coated Ti alloy implants can harbor bacteria that lead to more severe infection and reduced osteointegration compared with uncoated Ti alloys [58,59]. The results of this study are remarkable in that $Si_3N_4$ effectively eliminated bacterial infection while promoting osteointegration, without the necessity of a bioactive coating.

Other researchers have found that $Si_3N_4$ possesses excellent in vivo characteristics. For instance, using an adult rabbit model Howlett et al. implanted porous $Si_3N_4$ plugs into femoral marrow cavities and noted that mature bone completely enclosed the implants within 4 months post-operative, and remained unchanged for the rest of the life of the animal [1]. Neumann (2004) performed a comparative evaluation of $Al_2O_3$ and $Si_3N_4$ implants surgically placed into the femurs of New Zealand white male rabbits and used digital imaging and conventional histological analyses to compare bony apposition 8 weeks post-operative. The digital image analysis showed no statistical differences, but conventional histology demonstrated significantly lower bone–implant contact for $Al_2O_3$ compared with $Si_3N_4$ [8]. Later Neumann et al. implanted $Si_3N_4$ plates and screws into the frontal bone defects of three mini-pigs and performed histological examinations 3 months post-operatively. They found that bone healing was complete in all animals, and that the observed new bone was in direct contact with the implants [11]. In two more recent studies Guedes e Silva et al. examined osteointegration of silicon nitride in rabbit tibiae for 8 weeks using classic histology and scanning electron microscopy [9,14]. They observed no adverse tissue reactions. New bone was generated mainly in cortical areas in good apposition to the implants, and growth rates appeared

to accelerate 4 weeks after surgery. They also found that $Si_3N_4$ encouraged osteoconduction, as is evident by bone bridge formation to the implant surface. The body of evidence presented in these prior studies demonstrates that $Si_3N_4$ is not only biocompatible but serves as an excellent scaffold for osteointegration and osteoconduction. The results of the present study are therefore consistent with these prior in vivo observations.

Limitations of the present study relate to the fact that only three biomaterials were tested with a single strain of Gram-positive bacteria in a rodent model. Different results may be obtained with other strains and/or species of bacteria, biomaterials, implant surface characteristics, and animal models. Macroscale level investigations, such as our study, may also be insufficient to examine microbial adhesion to inert surfaces; higher resolution tools such as atomic force microscopy may be necessary to illustrate differences in nanoscale adhesion that correlate with the pathogenicity of bacteria [60]. Finally, our study did not show whether strong new bone formation and anti-bacterial behavior are specific to $Si_3N_4$ or whether these material properties are common to other orthopedic ceramics, such as alumina and zirconia [61]. Previous studies comparing Ti alloys and zirconia ceramics have not shown significant differences between these biomaterials in terms of biofilm formation and bacterial adhesion [62,63]. Nonetheless, future data are needed to validate the present observations in a larger animal model under physiological force environments and to determine whether or not the observed results are specific to $Si_3N_4$.

The present study suggests that $Si_3N_4$ may have especially favorable material properties for skeletal reconstruction. In addition to the advantages suggested in our study, $Si_3N_4$ implants can be manufactured in both porous and highly polished configurations that are useful in designing orthopedic bearings, fusion devices, and related implants [13,64]. Specific surface modifications of $Si_3N_4$ may prove yet more advantageous for biomedical applications. For example, the formation of stable complexes of $Si_3N_4$ with silver nanoparticles has been demonstrated [65]. The suppression of bacteria by $Si_3N_4$ observed in this study and the known bactericidal properties of silver ions [66,67] may prove valuable in developing antibacterial therapies based on biomaterial composition. Porous $Si_3N_4$ is also amenable to single molecule sensing [68], and the mapping of individual cells [69] and the material surface can be modified to promote the immobilization of selective proteins [70]. These data and the encouraging findings in the present study suggest that $Si_3N_4$ warrants further investigation as a promising new biomaterial for orthopedic implants.

## 5. Conclusions

The present in vivo study was carried out to examine the propensity for infection and the osteointegrative behavior of different commercially available biomaterials in the presence or absence of *S. epidermidis*. The results demonstrated that $Si_3N_4$ has substantially improved antibacterial and osteoinductive properties compared with Ti and PEEK. With or without bacterial inoculation, $Si_3N_4$ implants proved to be anti-infective, with greater bone formation within the surgical defect area and a significantly greater implant push-out strength relative to similar implants made of Ti or PEEK. The results further suggest that $Si_3N_4$ is an effective bacteriostatic material. In contrast to Ti and PEEK, no infection was observed with bacteria-inoculated $Si_3N_4$ implants at the conclusion of the study, whereas both Ti and PEEK implants maintained their septic states. This research provides insight for surgeons on the differential properties of biomaterials in terms of inhibiting bacterial colonization and promoting osseous fixation. Such knowledge should provide better clinical outcomes and lead to an improved patient quality of life and longevity.

## 6. Disclosures

B.S.B. is advisory surgeon to Amedica, developer of synthetic silicon nitride for orthopedic applications, and serves on the Board of Directors of Amedica, Salt Lake City, UT. A.A.P. is consulting design surgeon for Amedica. M.N.R. and T.J.W. have no disclosures concerning this article.

## Acknowledgements

The authors thank Alan Lakshminarayanan Ph.D., Senior Director of Research and Development, Bryan McEntire MBA, Chief Technology Officer, Ryan Bock Ph.D., Research Scientist, all of Amedica Corporation (Salt Lake City, UT), and Steve C. Friedman, Senior Editor, Department of Orthopedic Surgery, University of Missouri, for their kind assistance with this paper.

## References

[1] Howlett CR, McCartney E, Ching W. The effect of silicon nitride ceramic on rabbit skeletal cells and tissue. Clin Orthop Relat Res 1989;224:293–304.
[2] Zhou YS, Ohashi M, Tomita N, Ikeuchi K, Takashima K. Study on the possibility of silicon nitride—silicon nitride as a material for hip prostheses. Mater Sci Eng C 1997;5(2):125–9.
[3] Kue R, Sohrabi A, Nagle D, Frondoza C, Hungerford D. Enhanced proliferation and osteocalcin production by human osteoblast-like MG63 cells on silicon nitride ceramic discs. Biomaterials 1999;20(13):1195–201.
[4] Amaral M, Lopes MA, Santos JD, Silva RF. Wettability and surface charge of $Si_3N_4$–bioglass composites in contact with simulated physiological liquids. Biomaterials 2002;23(20):4123–9.
[5] Amaral M, Lopes M, Silva RF, Santos JD. Densification route and mechanical properties of $Si_3N_4$–bioglass biocomposites. Biomaterials 2002;23(3):857–62.
[6] Amaral M, Costa MA, Lopes MA, Silva RF, Santos JD, Fernandes MH. $Si_3N_4$–bioglass composites stimulate the proliferation of MG63 osteoblast-like cells and support the osteogenic differentiation of human bone marrow cells. Biomaterials 2002;23(24):4897–906.
[7] Guedes e Silva CC, Higa OZ, Bressiani JC. Cytotoxic evaluation of silicon nitride-based ceramics. Mater Sci Eng C 2004;24(5):643–6.
[8] Neumann A, Kramps M, Ragoß C, Maier HR, Jahnke K. Histological and microradiographic appearances of silicon nitride and aluminum oxide in a rabbit femur implantation model. Materialwissenschaft und Werkstofftechnik 2004;35(9):569–73.
[9] Guedes e Silva CC, König B, Carbonari MJ, Yoshimoto M, Allegrini S, Bressiani JC. Bone growth around silicon nitride implants – an evaluation by scanning electron microscopy. Mater Char 2008;59(9):1339–41.
[10] Guedes e Silva CC, Cristina da Silva Rigo E, Marchi J, Helena de Almeida Bressiani A, Bressiani JC. Hydroxyapatite coating on silicon nitride surfaces using the biomimetic method. Mater Res 2008;11(1):47–50.
[11] Neumann A, Unkel C, Werry C, Herborn CU, Maier HR, Ragoss C, et al. Prototype of a silicon nitride ceramic-based miniplate osteofixation system for the midface. Otolaryngol Head Neck Surg 2006;134(6):923–30.
[12] Neumann A, Reske T, Held M, Jahnke K, Ragoss C, Maier HR. Comparative investigation of the biocompatibility of various silicon nitride ceramic qualities in vitro. J Mater Sci Mater Med 2004;15(10):1135–40.
[13] Bal BS, Rahaman MN. Orthopedic applications of silicon nitride ceramics. Acta Biomater 2012;8(8):2889–98.
[14] Guedes e Silva CC, Konig B, Carbonari MJ, Yoshimoto M, Allegrini S, Bressiani JC. Tissue response around silicon nitride implants in rabbits. J Biomed Mater Res A 2008;84(2):337–43.
[15] Zhang W, Titze M, Cappi B, Wirtz DC, Telle R, Fischer H. Improved mechanical long-term reliability of hip resurfacing prostheses by using silicon nitride. J Mater Sci Mater Med 2010;21(11):3049–57.
[16] Dabrowski B, Swieszkowski W, Godlinski D, Kurzydlowski KJ. Highly porous titanium scaffolds for orthopaedic applications. J Biomed Mater Res B Appl Biomater 2010;95(1):53–61.
[17] Pohler OE. Unalloyed titanium for implants in bone surgery. Injury 2000;31(Suppl. 4):7–13.
[18] Pokorny D, Fulin P, Slouf M, Jahoda D, Landor I, Sosna A. Polyetheretherketone (PEEK). Part II: Application in clinical practice. Acta Chir Orthop Traumatol Cech 2010;77(6):470–8.
[19] Kurtz SM, Devine JN. PEEK biomaterials in trauma, orthopedic, and spinal implants. Biomaterials 2007;28(32):4845–69.
[20] Toth JM, Wang M, Estes BT, Scifert JL, Seim HB, Turner AS. Polyetheretherketone as a biomaterial for spinal applications. Biomaterials 2006;27(3):324–34.
[21] Matar WY, Jafari SM, Restrepo C, Austin M, Purtill JJ, Parvizi J. Preventing infection in total joint arthroplasty. J Bone Joint Surg Am 2010;92(Suppl. 2):36–46.
[22] Darouiche RO. Treatment of infections associated with surgical implants. N Engl J Med 2004;350(14):1422–9.

[23] Katsikogianni M, Missirlis YF. Concise review of mechanisms of bacterial adhesion to biomaterials and of techniques used in estimating bacteria–material interactions. Eur Cell Mater 2004;8:37–57.
[24] Antoci V, Adams CS, Parvizi J, Davidson HM, Composto RJ, Freeman TA, et al. The inhibition of *Staphylococcus epidermidis* biofilm formation by vancomycin-modified titanium alloy and implications for the treatment of periprosthetic infection. Biomaterials 2008;29(35):4684–90.
[25] Arciola CR, Visai L, Testoni F, Aricola S, Campoccia D, Speziale P, et al. Concise survey of *Staphylococcus aureus* virulence factors that promote adhesion and damage to peri-implant tissues. Int J Artif Organs 2011;34(9):771–80.
[26] Iturriza I, Castro F, Fuentes M. Sinter and sinter-HIP of silicon nitride ceramics with yttria and alumina additions. J Mater Sci 1989;24(6):2047–56.
[27] ASTM International. Standard practice for surface wettability of coatings, substrates, and pigments by advancing contact angle measurement, ASTM D7334-08. West Conshohocken, PA: ASTM International; 2008.
[28] Bosch C, Melsen B, Vargervik K. Importance of the critical-size bone defect in testing bone-regenerating materials. J Craniofac Surg 1998;9(4):310–6.
[29] Rohrer MD, Schubert CC. The cutting–grinding technique for histologic preparation of undecalcified bone and bone-anchored implants. Improvements in instrumentation and procedures. Oral Surg Oral Med Oral Pathol 1992;74(1):73–8.
[30] Donath K, Breuner G. A method for the study of undecalcified bones and teeth with attached soft tissues. The Sage–Schliff (sawing and grinding) technique. J Oral Path 1982;11(4):318–26.
[31] Umoh JU, Sampaio AV, Welch I, Pitelka V, Goldberg HA, Underhill TM, et al. In vivo micro-CT analysis of bone remodeling in a rat calvarial defect model. Phys Med Biol 2009;54(7):2147–61.
[32] Fogolari F, Brigo A, Molinari H. The Poisson–Boltzmann equation for biomolecular electrostatics: a tool for structural biology. J Mol Recognit 2002;15(6):377–92.
[33] Brown AM. A step-by-step guide to non-linear regression analysis of experimental data using a Microsoft Excel spreadsheet. Comput Methods Programs Biomed 2001;65(3):191–200.
[34] Jarman-Smith M. Evolving uses for implantable PEEK and PEEK based compounds. Med Device Technol 2008;19(6):12–5.
[35] Smith JS, Shaffrey CI, Sansur CA, Berven SH, Fu K-MG, Broadstone PA, et al. Rates of infection after spine surgery based on 108,419 procedures: a report from the Scoliosis Research Society Morbidity and Mortality Committee. Spine 2011;36(7):556–63.
[36] Schoenfeld AJ, Ochoa LM, Bader JO, Belmont PJ. Risk factors for immediate postoperative complications and mortality following spine surgery: a study of 3475 patients from the National Surgical Quality Improvement Program. J Bone Joint Surg Am 2011;93(17):1577–82.
[37] Collins I, Wilson-MacDonald J, Chami G, Burgoyne W, Vineyakam P, Berendt T, et al. The diagnosis and management of infection following instrumented spinal fusion. Eur Spine J 2008;17(3):445–50.
[38] An YH, Friedman RJ. Concise review of mechanisms of bacterial adhesion to biomaterial surfaces. J Biomed Mater Res 1998;43(3):338–48.
[39] Heilmann C. Adhesion mechanisms of staphylococci. Adv Exp Med Biol 2011;715:105–23.
[40] Eliaz N, Ritman-Hertz O, Aronov D, Weinberg E, Shenhar Y, Rosenman G, et al. The effect of surface treatments on the adhesion of electrochemically deposited hydroxyapatite coating to titanium and on its interaction with cells and bacteria. J Mater Sci Mater Med 2011;22(7):1741–52.
[41] Rupp F, Haupt M, Eichler M, Doering C, Klostermann H, Scheideler L, et al. Formation and photocatalytic decomposition of a pellicle on anatase surfaces. J Dent Res 2012;91(1):104–9.
[42] Patel JD, Ebert M, Ward R, Anderson JM. *S. epidermidis* biofilm formation: effects of biomaterial surface chemistry and serum proteins. J Biomed Mater Res A 2007;80(3):742–51.
[43] MacKintosh EE, Patel JD, Marchant RE, Anderson JM. Effects of biomaterial surface chemistry on the adhesion and biofilm formation of *Staphylococcus epidermidis* in vitro. J Biomed Mater Res A 2006;78(4):836–42.
[44] Jou C-H, Yuan L, Lin S-M, Hwang MC, Chou WL, Yu DG, et al. Biocompatibility and antibacterial activity of chitosan and hyaluronic acid immobilized polyester fibers. J Appl Polym Sci 2007;104(1):220–5.
[45] Ikeda T, Hirayama H, Yamaguchi H, Tazuke S, Watanabe M. Polycationic biocides with pendant active groups: molecular weight dependence of antibacterial activity. Antimicrob Agents Chemother 1986;30(1):132–6.
[46] Shi Z, Neoh KG, Kang ET, Poh C, Wang W. Bacterial adhesion and osteoblast function on titanium with surface-grafted chitosan and immobilized RGD peptide. J Biomed Mater Res A 2008;86(4):865–72.
[47] Hamilton V, Yuan Y, Rigney DA, Chesnutt BM, Puckett AD, Ong JL, et al. Bone cell attachment and growth on well-characterized chitosan films. Polym Int 2007;56(5):641–7.
[48] Hunter A, Archer CW, Walker PS, Blunn GW. Attachment and proliferation of osteoblasts and fibroblasts on biomaterials for orthopaedic use. Biomaterials 1995;16(4):287–95.
[49] Boyan BD, Schwartz Z, Lohmann CH, Sylvia VL, Cochran DL, Dean DD, et al. Pretreatment of bone with osteoclasts affects phenotypic expression of osteoblast-like cells. J Orthop Res 2003;21(4):638–47.
[50] Martin JY, Schwartz Z, Hummert TW, Schraub DM, Simpson J, Lankford J, et al. Effect of titanium surface roughness on proliferation, differentiation, and protein synthesis of human osteoblast-like cells (MG63). J Biomed Mater Res 1995;29(3):389–401.
[51] Deligianni DD, Katsala N, Ladas S, Sotiropoulou D, Amedee J, Missirlis YF. Effect of surface roughness of the titanium alloy Ti-6Al-4V on human bone marrow cell response and on protein adsorption. Biomaterials 2001;22(11):1241–51.
[52] Webster TJ, Ergun C, Doremus RH, Siegel RW, Bizios R. Enhanced functions of osteoblasts on nanophase ceramics. Biomaterials 2000;21(17):1803–10.
[53] Lincks J, Boyan BD, Blanchard CR, Lohmann CH, Liu Y, Cochran DL, et al. Response of MG63 osteoblast-like cells to titanium and titanium alloy is dependent on surface roughness and composition. Biomaterials 1998;19(23):2219–32.
[54] Zhao G, Raines AL, Wieland M, Schwartz Z, Boyan BD. Requirement for both micron- and submicron scale structure for synergistic responses of osteoblasts to substrate surface energy and topography. Biomaterials 2007;28(18):2821–9.
[55] Sagomonyants KB, Jarman-Smith ML, Devine JN, Aronow MS, Gronowicz GA. The in vitro response of human osteoblasts to polyetheretherketone (PEEK) substrates compared to commercially pure titanium. Biomaterials 2008;29(11):1563–72.
[56] Wang H, Xu M, Zhang W, Kwok DT, Jiang J, Wu Z, et al. Mechanical and biological characteristics of diamond-like carbon coated poly aryl-ether-ether-ketone. Biomaterials 2010;31(32):8181–7.
[57] Olivares-Navarrete R, Gittens RA, Schneider JM, Hyzy SL, Haithcock DA, Ullrich PF, et al. Osteoblasts exhibit a more differentiated phenotype and increased bone morphogenetic protein production on titanium alloy substrates than on poly-ether-ether-ketone. Spine J 2012;12(3):265–72.
[58] Vogely HC, Oosterbos CJ, Puts EW, Nijhof MW, Nikkels PG, Fleer A, et al. Effects of hydroxyapatite coating on Ti–6Al–4V implant-site infection in a rabbit tibial model. J Orthop Res 2000;18(3):485–93.
[59] Oosterbos CJ, Vogely HC, Nijhof MW, Fleer A, Verbout AJ, Tonino AJ, et al. Osseointegration of hydroxyapatite-coated and noncoated Ti6Al4V implants in the presence of local infection: a comparative histomorphometrical study in rabbits. J Biomed Mater Res 2002;60(3):339–47.
[60] Park B-J, Haines T, Abu-Lail NI. A correlation between the virulence and the adhesion of *Listeria monocytogenes* to silicon nitride: an atomic force microscopy study. Colloids Surf B Biointerfaces 2009;73(2):237–43.
[61] Hernigou P, Bahrami T. Zirconia and alumina ceramics in comparison with stainless-steel heads. Polyethylene wear after a minimum ten-year follow-up. J Bone Joint Surg Br 2003;85(4):504–9.
[62] Schwartz Z, Raz P, Zhao G, Barak Y, Tauber M, Yao H, et al. Effect of micrometer-scale roughness of the surface of Ti6Al4V pedicle screws in vitro and in vivo. J Bone Joint Surg Am 2008;90(11):2485–98.
[63] Al-Ahmad A, Wiedmann-Al-Ahmad M, Faust J, Bächle M, Follo M, Wolkewitz M, et al. Biofilm formation and composition on different implant materials in vivo. J Biomed Mater Res B Appl Biomater 2010;95(1):101–9.
[64] Bal BS, Khandkar A, Lakshminarayanan R, Clarke I, Hoffman AA, Rahaman MN. Fabrication and testing of silicon nitride bearings in total hip arthroplasty: winner of the 2007 "HAP" PAUL award. J Arthroplasty 2009;24(1):110–6.
[65] Afanasiev SA, Tsapko LP, Kurzina IA, Chuhlomina LN, Babokin VE. Effect of model biological media on stability of complex of silver nanoparticles applied onto silicon nitride substrate. Bull Exp Biol Med 2010;150(1):160–4.
[66] Fiedler J, Kolitsch A, Kleffner B, Henke D, Stenger S, Brenner RE. Copper and silver ion implantation of aluminium oxide-blasted titanium surfaces: proliferative response of osteoblasts and antibacterial effects. Int J Artif Organs 2011;34(9):882–8.
[67] Tseng K-H, Liao C-Y, Tien D-C. Control release of bactericidal ion by an electronically driven system. J Nanosci Nanotechnol 2011;11(12):10750–4.
[68] Vadillo-Rodriguez V, Busscher HJ, Norde W, De Vries J, Dijkstra RJ, Stokroos I, et al. Comparison of atomic force microscopy interaction forces between bacteria and silicon nitride substrata for three commonly used immobilization methods. Appl Environ Microbiol 2004;70(9):5441–6.
[69] Shirshov YM, Snopok BA, Samoylov AV, Kiyanovski AP, Venger EF, Nabok AV, et al. Analysis of the response of planar polarization interferometer to molecular layer formation: fibrinogen adsorption on silicon nitride surface. Biosens Bioelectron 2001;16(6):381–90.
[70] Diao J, Ren D, Engstrom JR, Lee KH. A surface modification strategy on silicon nitride for developing biosensors. Anal Biochem 2005;343(2):322–8.